

Kinetic Factors Determining Specific Features of Solid Phase Formation in Dichlorosilane Oxidation

V. V. Azatyan, A. G. Merzhanov, N. M. Rubtsov, G. I. Tsvetkov, and V. I. Chernysh

Institute of Structural Macrokinetics, Russian Academy of Sciences, Chernogolovka, Moscow oblast, Russia

Received February 13, 2002

Abstract—Experimental data on the kinetic regularities of aerosol SiO₂ formation in the course of dichlorosilane oxidation by oxygen at different initial pressures, compositions of the reaction mixture, and temperatures ranging from 380 to 578 K are presented. It is shown that the regularities of the process, including the specific feature of the transition from the regime of solid phase formation in the form of a film to the regime of aerosol formation can be explained on the basis of the Volmer–Weber–Frenkel–Zeldovich nucleation theory taking into account the branched chain nature of the reaction. The conditions for the transition of chain combustion into the regime of chain–thermal explosion almost coincide with the conditions of intensive formation of aerosol. The SF₆ additives inhibit the process and thereby increase the dispersity of aerosol and the minimal pressure of its formation.

INTRODUCTION

The broad applicability of thin and ultradispersed powders is attributable to their unusual properties due to tremendous specific surface area and specific features of their microstructure [1–3]. The most promising method for the preparation of ultradispersed powders of silicon oxide and oxynitride is deposition from the gas phase using the oxidation and pyrolysis of silane and its derivatives (see, for instance, [4–11]). A distinctive feature of these processes is the existence of two regimes of solid phase formation, one of which leads to film formation, and the other leads to the formation of aerosol [7–11]. The elucidation of the conditions for the realization of these regimes and the specific features of the process transition from one regime to the other is of great interest for both the theory of heterophaseous chemical processes and for practice. Each of the cited forms of the solid product (aerosol and film) has its own applications, and this circumstance is responsible for the high standards in the technologies of their preparation. For instance, in the preparation of solid dielectrics and protective layers, the formation of aerosol particles makes the film quality substantially worse.

A change in the regimes of phase formation occurs in narrow ranges of initial parameters (composition, temperature, and pressure) of the reaction system [7–11]. These regimes differ both in the nature of the solid product and in the kinetic characteristics of the reaction [7]. The transfer to the regime of aerosol formation corresponds to a drastic acceleration of the process. The occurrence of the process in each of the cited kinetic regimes is determined by the concentrations of gas-phase components, temperature, the composition of the adsorption layer of the reactor surface, and by the preliminary chemical treatment of the surface [7].

The mechanism of transfer from one regime of phase formation to another is practically unknown. It has been found [11] that it is chemical reaction rather than nucleus growth that limits the process of aerosol formation in both the oxidation of dichlorosilane (DCS) and film formation in silane oxidation [7].

It has also been found [8] that the kinetic regimes of phase formation, which accompanies the combustion of dichlorosilane–oxygen mixtures at 293 K, differ depending on whether spontaneous ignition occurs or combustion is initiated artificially. However, the temperature range for the conditions for the realization of these regimes has not been studied. It followed from the branched chain nature of the oxidation of volatile hydrides, from the specific dependence of the rate of this class of reactions on temperature, and from the existence of various kinetic regimes of chain combustion processes [12, 13] that the temperature dependence of the rate of solid phase formation also has a specific character. The chain nature of the reaction also indicates the sensitivity of the kinetics of phase formation and the properties of the solid phase to the effect of inhibitors and promoters.

This work had the following goals:

- (a) To determine the nature of the dependence of the rate of aerosol SiO₂ formation on the initial conditions using DCS oxidation in the regime of self-ignition as an example;
- (b) To determine the specific features of the transition of DCS oxidation process from the regime of SiO₂ film formation to the regime of aerosol formation;
- (c) To determine kinetic factors responsible for the transition of one regime of phase formation to another and the aerosol dispersity based on the modern conception of nonisothermal radical chain process (RCP).

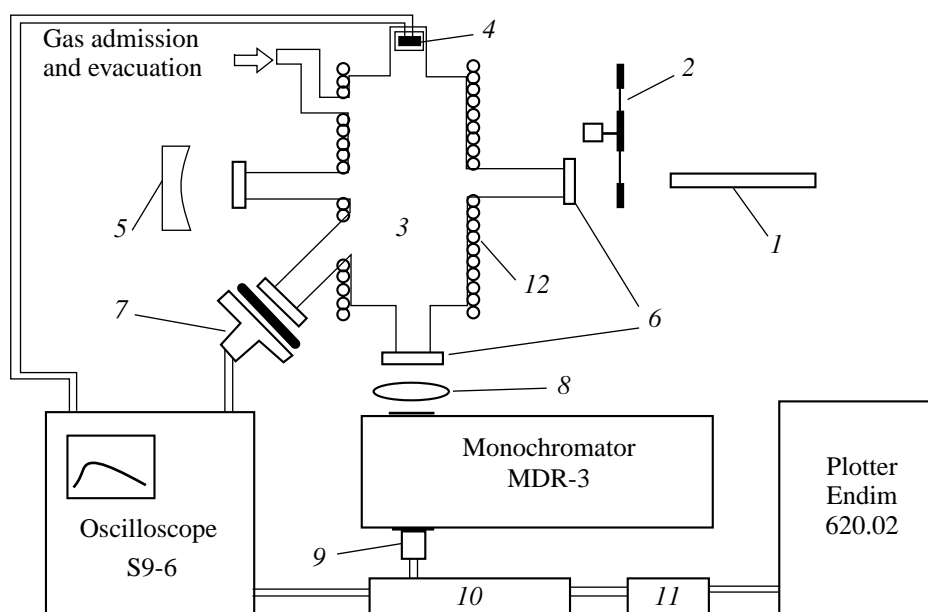


Fig. 1. Schematic of the experimental setup. (1) He-Ne laser; (2) shutter; (3) reactor; (4) piezoelectric pressure transducer; (5) spherical mirror; (6) optical windows; (7) FEU-39 equipped with an UFS-1 light filter; (8) collimator; (9) FEU-71; (10) amplifiers UZ-29 and U2-8; (11) microvoltmeter F-136; (12) electric furnace equipped with a thermocouple and a temperature controller.

EXPERIMENTAL

The static vacuum setup describe in [14] was used. The reaction was carried out in the thermostated quartz reactor with a diameter of 4 cm and a length of 20 cm (Fig. 1) in the temperature range 383–573 K and pressure ranging from 0.5 to 20.0 Torr. Temperature was controlled and measured using a KVA-501 temperature-sensing device with an accuracy of ± 0.5 K. The optical quartz windows of the reactor were polished after every 20 ignitions.

Aerosol formation was registered using laser beam light scattering at an angle of 90° on the SiO_2 particles. The scheme of registration was described in [11]. The LGN-207A laser beam (632.8 nm) passing through a reactor was reflected by a spherical mirror ($R = 2$ m) and focused back onto the laser cavity. The intensity of laser radiation was modulated with a mechanical chopper with a frequency of 3.3 kHz. The scattered light was focused on the entrance slit of a MDR-3 monochromator equipped with grating that had 600 grooves per 1 mm and registered with a FEU-71 photomultiplier tube with a spectral sensitivity in the range 200–800 nm. The signal from FEU-71 was supplied to the inlet of UZ-29 and U2-8 alternating current amplifiers. Then, the alternating signal passed from the U2-8 amplifier to an S9-6 double-beam memory oscilloscope. The envelope of the sinusoidal signal with a frequency of 3.3 kHz was the kinetic curve describing changes in the amount of aerosol, which scattered radiation in the region of the reaction volume cut off by the monochromator slit. A signal from a PD-7 piezoelectric transducer was supplied to the second beam of the oscilloscope. The oscilloscope was triggered in the anticipatory mode using

FEU-39 (with a spectral sensitivity of 200–600 nm) equipped with UFS-1 light filters. The U2-8 amplifier also made it possible to obtain the envelope of the alternating signal at the output; that is, a direct signal with a time constant of ~ 0.1 s was obtained in this case. This amplifier also enabled synchronous signal detection. The light intensity of probing radiation scattered by aerosol served as a measure of the amount of aerosol formed as in [11]. With this goal, the direct signal was supplied from U2-8 to an F-136 microvoltmeter and then to an Endim 620.02 plotter.

The distribution of aerosol particles over sizes was determined using a Fritsch particle sizer (Germany) after aerosol discharging from the reactor.

The lower limit of self-ignition (P_1) was determined by the crossover method as a mean of two pressures, at the higher of which the mixture ignited and at the lower of which it did not.

The reactor was evacuated to 6×10^{-4} Torr and controlled the residual pressure with a VIT-2 vacuum gauge. O_2 and SF_6 were of chemical purity grade. The purity of DCS was controlled by spectrophotometry. The preliminarily prepared mixture of DCS with oxygen (and, if necessary, with SF_6) was admitted from the bypass header into the reactor while controlling the pressure with a VDG-1 gas-discharge vacuum gauge. The mixtures 11, 13, and 14% DCS + O_2 were used, as well as the mixtures 11% DCS + 4.8% SF_6 + O_2 and 11% DCS + 10% SF_6 + O_2 .

RESULTS AND DISCUSSION

Points in Figs. 2–5 show experimental data on the dependence of the maximal intensity of light scattering (I_p) on the initial pressure of the mixture (P_0) in the course of DCS combustion at different initial temperatures (T_0). The direct signal was registered (the constant of the registration channel was 0.1 s). The values of I_p are divided by the partial pressure of DCS (ϕP_0 , where ϕ is the molar fraction of DCS) to reduce data to identical conditions. The curves in the figures show the results of calculations of the maximal rate of phase formation ($Y_{8,\max}$ is the dimensionless concentration of aerosol). Figure 4 shows the values of the increase in the temperature (ΔT) due to self-heating. In the case of the complex shape of the scattering signal due to mixing the aerosol cloud with convective gas flows (see [11]), the first-appeared maximum of the scattering signal, which characterizes the amount of aerosol in the volume immediately before ignition, was taken as a maximum value I_p . Note that the maximal intensities obtained in the registration of the alternating current (with a time constant equal to 300 μ s) correlate with those shown in Figs. 2–5 (similarly to the case of initiated ignition [11]). Special runs were carried out to show that the chemiluminescence of DCS oxidation reaction cannot be observed using this method in this spectral range, because chemiluminescence is not modulated and the registered signal completely refers to light scattered by aerosol.

Comparison of data presented in Figs. 2 and 3 and those presented in [11] suggests that the dependence of I_p on the total pressure at the instant of self-ignition is sharper than in the case of initiated ignition when this dependence had the form of an S-shaped curve. With an increase in the initial temperature (T_0), the amount of aerosol formed in the volume noticeably decreased both in the absence and in the presence of SF₆ additives (Figs. 2, 3, 5). With an increase in the amount of SF₆ additive, the initial pressure (P_0) corresponding to the beginning of aerosol formation increases.

Because $\Delta P/P_0 = \Delta T/T_0$ in a closed volume when moles of the gaseous mixture change insignificantly, $\Delta T = \Delta P T_0/P_0$ (where ΔT and ΔP are changes in temperature due to self-heating and pressure, respectively, in self-ignition). Therefore, the signal from the pressure transducer characterizes the value of self-heating. Figure 4 shows that a drastic increase in the temperature due to self-heating and an increase in the amount of aerosol formed is observed in the same interval of P_0 values, and this interval corresponds to the transfer from chain combustion with low self-heating to the regime of chain–thermal explosion characterized by abrupt intensification of combustion (ΔP increases in a step and ignition starts to be accompanied with a distinctive flick).

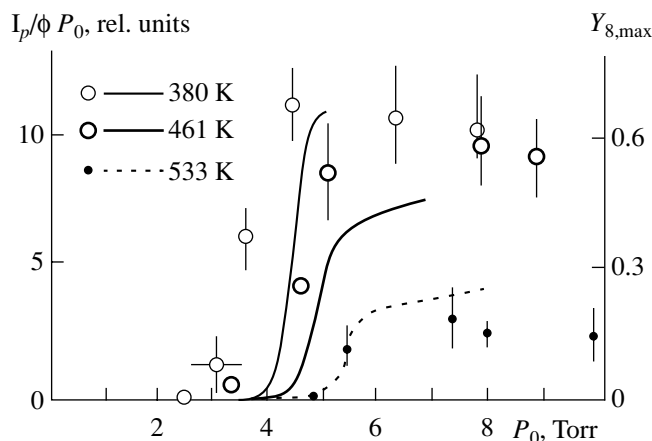


Fig. 2. Dependence of the maximal concentration of aerosol on P_0 for the mixture 14% DCS in O₂. Points refer to the experiment and solid lines refer to the calculation of $Y_{8,\max}$. Parameters (for dimensions, see text) $k_0 = 10^{-6}$, $k_1^0 = 4 \times 10^{-11}$, $\varepsilon = 3300$, $k_2^0 = 10^{-12}$, $k_3 = 10^{-12}$, $k_5^0 = 5 \times 10^{-13}$, $k_{-5} = 4 \times 10^4$, $t_0 = 0$, $t_1 = N = 6000$, t_0 and t_1 are limits of integration, and N is the number of integration steps. The values of P_1 (Torr) used in calculations of $k_{\text{het}}^{\text{eff}}$ are P_1 (380 K) = 1.5 ($k_{\text{het}}^{\text{eff}} = 81 \text{ s}^{-1}$), P_1 (461 K) = 1.1 ($k_{\text{het}}^{\text{eff}} = 205 \text{ s}^{-1}$), and P_1 (533 K) = 0.9 ($k_{\text{het}}^{\text{eff}} = 380 \text{ s}^{-1}$).

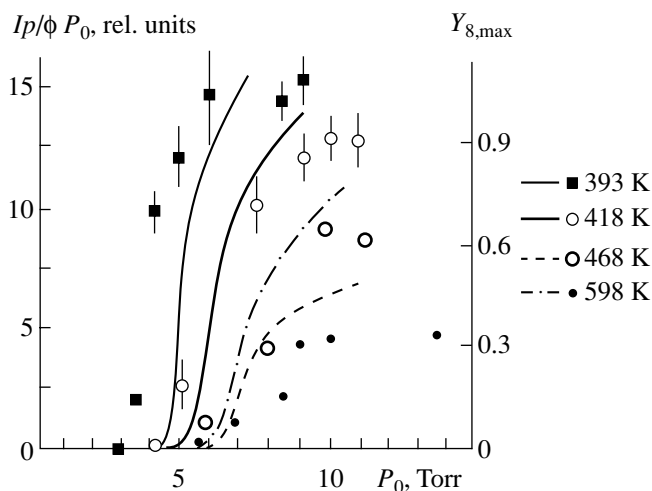


Fig. 3. Dependences of I_p on P_0 for the mixture 10.5% DCS in O₂. Points refer to the experiment and solid lines refer to the calculation of $Y_{8,\max}$. The values of parameters are the same as in Fig. 2. The values of P_1 (Torr) are P_1 (393 K) = 2.55 ($k_{\text{het}}^{\text{eff}} = 120 \text{ s}^{-1}$), P_1 (418 K) = 1.7 ($k_{\text{het}}^{\text{eff}} = 131 \text{ s}^{-1}$), P_1 (468 K) = 1.4 ($k_{\text{het}}^{\text{eff}} = 175 \text{ s}^{-1}$), and P_1 (598 K) = 1.05 ($k_{\text{het}}^{\text{eff}} = 360 \text{ s}^{-1}$).

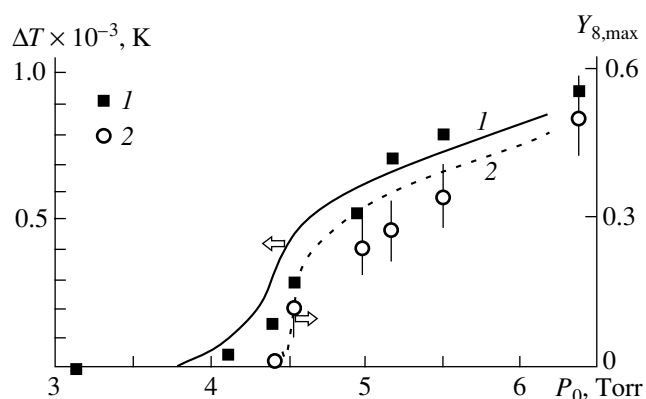


Fig. 4. Dependences of ΔT (1) and I_p (2) on P_0 for the mixture 13% DCS + O_2 at 473 K. Points refer to the experiment and solid lines refer to the calculation of $Y_{8,max}$ and ΔT . The values of parameters are the same as in Fig. 2. P_1 (473 K) = 1.01 Torr ($k_{het}^{eff} = 180 \text{ s}^{-1}$).

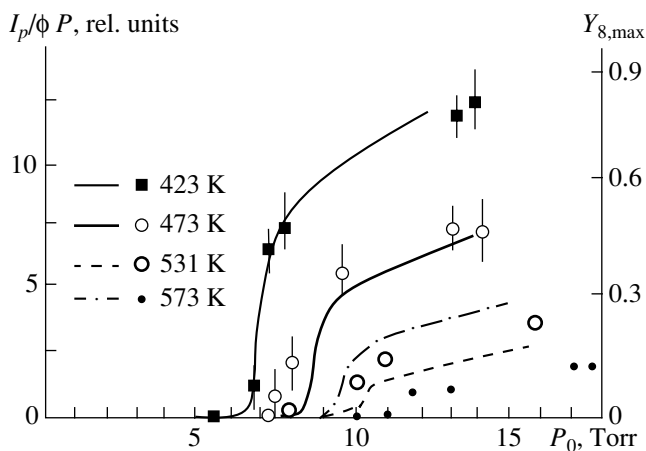


Fig. 5. Dependences of I_p on P_0 for the mixture 11% DCS + O_2 + 4.8% SF_6 . Points refer to the experiment and solid lines refer to the calculation of $Y_{8,max}$. The values of parameters are the same as in Fig. 2. The values of P_1 (Torr) are P_1 (423 K) = 2.05 ($k_{het}^{eff} = 170 \text{ s}^{-1}$), P_1 (473 K) = 1.61 ($k_{het}^{eff} = 270 \text{ s}^{-1}$), P_1 (531 K) = 1.34 ($k_{het}^{eff} = 400 \text{ s}^{-1}$), and P_1 (573 K) = 1.4 ($k_{het}^{eff} = 550 \text{ s}^{-1}$).

Below, when we interpret the regularities of phase formation in the course of silane and DCS combustion, we will take into account that aerosol formation is a three-dimensional process and film formation is a two dimensional process (as was done in the Volmer–Weber–Frenkel–Zeldovich theory of nucleus growth [4, 15–17]). This approach leads to the following equations of the rates of aerosol formation J_3 and film formation J_2 of condensing particles **C** and **B**, respectively [4, 15–17] (see also [18, 19]):

$$J_3 = -dC/dt = \alpha(\rho S_3)(2\sigma M\pi)^{1/2}(C/RT)^2 \times \exp[-17.6(M/\rho)^2(\sigma/T)^3/\ln^2 S_3] = K_1 \exp(-\Delta/T^3), \quad (1)$$

$$J_2 = -dB/dt = K_2 B \times \exp[-8\pi\chi^2 M N_A / (\rho\sigma_2(RT)^2/\ln S_2)] = K_2 B \exp(-\delta/T^2), \quad (2)$$

where $S_3 = C/p_0(T)$ is the degree of oversaturation of **C** in the volume (C is the partial pressure of **C**, $p_0(T)$ is the equilibrium pressure of **C** vapors), S_2 is the degree of oversaturation of two-dimensional gas, B is the surface concentration of **B**, σ_2 is the width of the two-dimensional nucleus (10^{-7} cm), α is the condensation coefficient (the probability that the vapor molecule sticks to the surface of the complex upon colliding with it), ρ is the density ($\rho_B = \rho_C = 2 \text{ g/cm}^3$), σ is the surface tension (400 erg/cm^2 [20]), χ is the specific peripheral energy ($4 \times 10^{-5} \text{ erg/cm}^3$ [21, 22]), M is the molecular weight (100 g/mol), and N_A is the Avogadro number. The numeric coefficient in the exponent of Eq. (1) corresponds to the spherical form of the nucleus ($\alpha = 1$), $K_2 = K_1^{2/3}$ [11]. In Eqs. (1) and (2), condensing products are generally considered as different substances. A specific case is the same chemical composition of the aerosol and film.

Equations (1) and (2) of the condensation rate were obtained without considering the possibility of chain processes in the system. However, this does not exclude the applicability of these expressions to condensation occurring in the course of a branched chain reaction. In such a system, the dependence of the rate of phase formation on temperature and reactant concentrations is much stronger. Indeed, it is known [12, 23] that, in the course of developing chain combustion, the concentrations of intermediate species (in this case, **C** and **B**) and the rate of the overall process exponentially increase with an increase in the pressure of the reaction mixture even if the temperature is constant. In the case of the branched chain mechanism, the dependence of the process rate on temperature is much stronger as well [12, 13]. This is due to the fact that, in the regime of developing chain combustion, the concentrations of intermediate species **C** and **B** increase with temperature according to the double exponent law; that is, the temperature dependence of these values is the exponent containing the Boltzmann factor in the positive exponent.

The above specific character of the dependence of **C** and **B** on the initial pressure and temperature, as well as strong positive feedback between each of these concentrations and the temperature, is the reason for the apparent drastic enhancement of phase formation with an increase in P_0 in the narrow interval of its values (Figs. 2–5).

Let us consider the reason behind the abrupt transition of the phase formation process from the regime of phase formation to the regime of aerosol formation with an increase in P_0 and T_0 [7, 11]. The rate of aerosol formation, which is a three-dimensional process, depends on the concentration of phase-forming intermediate product and on pressure more strongly than the rate of the two-dimension process of film formation. Equations (1) and (2) also show this. Therefore, at low degrees of oversaturation, the J_3 value is lower than J_2 , and above a certain critical oversaturation it is higher than J_3 . At the same time, because the dependence of the rates of aerosol and film formation is enhanced by the branched chain character of the reaction, the difference between the dependences of J_3 and J_2 on the initial conditions is also enhanced. Therefore, with an increase in P_0 above a certain value, film formation abruptly changes for aerosol formation. The same is also true of the effect of T_0 : with an increase in T_0 , J_3 increases more rapidly than J_2 . As a result, film formation is replaced by aerosol formation above a certain value of T_0 .

Results presented in Figs. 2–4, which show a decrease in the final amount of aerosol with an increase in T_0 , can be explained by an increase in the equilibrium pressure of vapors of the forming solid phase and by condensation abatement. This is illustrated by Eq. (1): with an increase in T_0 , $p_0(T)$ increases resulting in a decrease in the value $S_3 = C/p_0(T)$ involved in the denominator of the exponential factor in Eq. (1). Correspondingly, the rate of critical nucleus formation (i.e., phase formation) decreases.

It follows from the branched chain character of the process that its kinetics can be controlled by inhibition and promotion. SF_6 was used as an inhibitor in this work [24]. Because inhibition leads to a decrease in the intensity of combustion and diminishes self-heating, it should be expected that the dispersity of aerosol will increase when SF_6 is added. Indeed, the dispersity of aerosol obtained in the presence of SF_6 is higher than in the absence of SF_6 , other conditions being the same. As can be seen from a comparison of Figs. 6a and 6b, the maximum of aerosol distribution is shifted toward lower sizes and the concentration of submicron particles increases in the presence of SF_6 .

Thus, when the specific features of nonisothermal branched chain processes are taken into account together with the dependences of the saturated vapor pressure on temperature and reactant concentrations, the main regularities of phase formation accompanying silane and DCS combustion can be explained. This approach is also applicable to phase formation in other process of chain combustion.

Taking into account the radical chain nature of DCS oxidation makes it possible to model the quantitative pattern of phase formation. The block of homogeneous reactions and their rate constants in the kinetic scheme

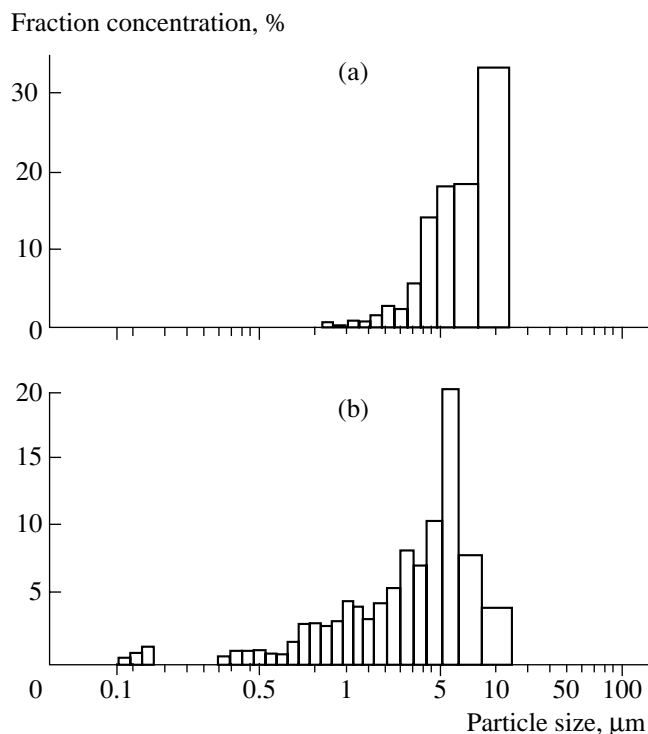


Fig. 6. Sedimentation patterns for the powder samples. $P_0 = 5$ Torr, $T_0 = 573$ K; (a) the mixture 20% DCS in O_2 and (b) 11% DCS + O_2 + 4.8% SF_6 .

involving aerosol formation is analogous to that reported in [11].

In calculations, we used dimensionless concentrations Y_i of the reaction components A_i normalized to the initial concentration of the initial substance (DCS) $A_1(Y_{1,0})$. The value $\tau = k_1^0 Y_{1,0} t$ was taken as the dimensionless time. Together with the reaction, we provide the values of the rate constants adopted in this work. The act of initiation is



The limiting step in the chain unit is the reaction of linear chain branching



$$k_1 = k_1^0 \exp(-\varepsilon/T), \quad k_1^0 = 4 \times 10^{-11} \text{ cm}^3 \text{ molecule}^{-1} \text{ s}^{-1}, \\ \varepsilon = 6.6/R \text{ kcal mol}^{-1} \text{ K}^{-1} [14].$$

The equation of heat balance was written in the following form [25]:

$$dT/dt = (Q/c_p \rho)w(T) - \alpha_1(L/c_p \rho)(T - T_0), \quad (3)$$

where Q is the thermal effect (170 kcal/mol [26]), c_p is the heat capacity of the mixture (8 cal mol⁻¹ K⁻¹ for O_2 [27]), α_1 is heat-transfer factor, L is the ratio of the surface area to the volume (cm⁻¹), $w(T)$ is the reaction rate, and T_0 is the initial temperature. The value of α_1 was

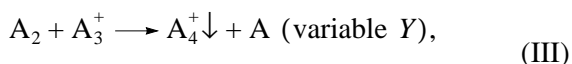
determined as described in [25]: $\alpha_1 = (L/r^2)\delta_1\lambda e$, where r is the reactor radius (4 cm), e is the natural logarithm base, δ_1 is the critical parameter (2.00), and λ is the thermal conductivity coefficient of the mixture (we assumed $\lambda = \lambda_{O_2}$ [27]). Since we considered only the qualitative pattern of phase formation, changes in c_p and Q in the course of the reaction were not considered.

Condensation on noncharged species formed in the course of chemiionization [28] plays an important role in the formation of a new phase. We assumed that chemiionization occurs in the exothermic reaction between active intermediate species A_2 and A_0 :



$$k_2 = k_2^0 e^{-2200/T} \text{ cm}^3 \text{ s}^{-1} \text{ molecule}^{-1}, \quad (\text{II})$$

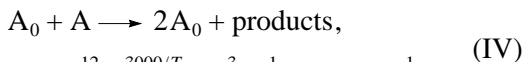
$$k_2^0 = 10^{-12} \text{ cm}^3 \text{ s}^{-1} \text{ molecule}^{-1},$$



$$k_3 = 10^{-12} \text{ cm}^3 \text{ s}^{-1} \text{ molecule}^{-1},$$

where $A_4^+\downarrow$ is the center of condensation. We took into account that the activation energy of exothermic ion-molecular reaction (III) is close to zero. The amount of substance condensed into aerosol is described by the variable Y_8 . The rate of aerosol accumulation, proportional to the specific rate of formation of three-dimensional nuclei Y_4 , is described by Eq. (1).

The scheme also involves nonlinear chain branching:

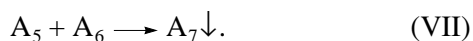
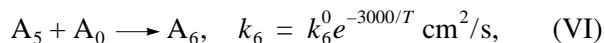


$$k_4 = 2 \times 10^{-12} e^{-3000/T} \text{ cm}^3 \text{ s}^{-1} \text{ molecule}^{-1}.$$

In contrast to [11], we assumed that the surface is uniform with respect to A_1 , whose adsorption and desorption are characterized by $k_5^0 = 10^{-12} \text{ cm}^3/\text{s}$ and $k_{-5} = 4 \times 10^4 \text{ cm}^2/\text{s}$, respectively [29]:



Species A_5 interact with A_0 from the volume. We also assumed that the flow of A_0 determining the heterogeneous chain termination is limited by the kinetics of their trapping by the surface. Film formation is represented by the steps whose sequence ends with A_7 condensation:



The growth rate of the layer of deposited coating is considered proportional to the specific rate of formation of two-dimensional nuclei Y_7 and described by Eq. (2). The concentration of A_6 on the surface is determined by the variable Y_9 .

The following set of equations corresponds to the above reaction scheme:

$$\begin{aligned} dY_0/d\tau &= Y_1 T k_0 / (k_1^0 \phi P \times 10^{19}) + 2Y_0 Y_1 e^{-\varepsilon/T} \\ &\quad - Y_0 T k_{\text{het}}^{\text{eff}} / (k_1^0 \phi P \times 10^{19}) + k_4^0 e^{-3000/T} Y_0 Y_1, \end{aligned} \quad (\text{4.1})$$

$$\begin{aligned} dY_1/d\tau &= -k_0 / (k_1^0 \phi P \times 10^{19}) Y_1 T - Y_0 Y_1 e^{-\varepsilon/T} \\ &\quad - k_5 Y_1 (1 - Y_5) / k_1^0 + k_{-5} T Y_5 / (k_1^0 \phi P \times 10^{19}), \end{aligned} \quad (\text{4.2})$$

$$\begin{aligned} dT/d\tau &= 10^4 \phi Y_0 Y_1 e^{-\varepsilon/T} \\ &\quad - 1200 T (T - T_0) / (k_1^0 \phi P \times 10^{19}), \end{aligned} \quad (\text{4.3})$$

$$\begin{aligned} dY_2/d\tau &= Y_0 Y_1 e^{-\varepsilon/T} - k_2^0 e^{-2200/T} Y_0 Y_3 / k_1^0 - k_3 Y_2 Y_3 / k_1^0, \end{aligned} \quad (\text{4.4})$$

$$dY_3/d\tau = k_2^0 e^{-2200/T} Y_0 Y_2 / k_1^0 - k_3 Y_2 Y_3 / k_1^0, \quad (\text{4.5})$$

$$dY_4/d\tau = 2k_3 Y_2 Y_3 / k_1^0 - J_3. \quad (\text{4.6})$$

$$\text{In } J_3 \text{ from (1) } C = Y_4, \quad S_3 = 0.98 Y_4$$

$$\times \phi P \times 10^3 / (\exp(-16500/T) T) \quad [\text{11}], \quad (\text{4.7})$$

$$\begin{aligned} dY_5/d\tau &= k_5 Y_1 (1 - Y_5) / k_1^0 \\ &\quad - k_{-5} T Y_5 / (k_1^0 \phi P \times 10^{19}) - k_6^0 e^{-3000/T} Y_5 Y_6 / k_1^0, \end{aligned}$$

$$\begin{aligned} dY_6/d\tau &= Y_0 Y_5 T k_{\text{het}}^{\text{eff}} / (k_1^0 \phi P \times 10^{19}) \\ &\quad - k_6^0 e^{-3000/T} Y_5 Y_6 / k_1^0, \end{aligned} \quad (\text{4.8})$$

$$dY_7/d\tau = k_6^0 e^{-3000/T} Y_5 Y_6 / k_1^0 - J_2, \quad (\text{4.9})$$

$$dY_8/d\tau = J_3, \quad (\text{4.10})$$

$$dY_9/d\tau = J_2. \quad (\text{4.11})$$

Here, ϕ is the molar fraction of fuel, P is pressure in Torr, $k_{\text{het}}^{\text{eff}}$ is the effective rate constant of heterogeneous chain termination whose value was determined from the values of P_1 and k_1 by analogy with [23]. The effect of solid phase formation on the process was neglected. This is one of the important reasons why this model and the model reported in [11] cannot pretend to describe the process characteristics quantitatively. The above statement is also applicable to the effect of soot on the oxidation and oxidative cracking of organic compounds, which is necessary for the quantitative description of the process.

In expression for J_2 from Eq. (2), $B = Y_7$, $S_2 = Y_7 \times 10^{10} \exp(-1500/T)$ [11].

As calculation shows, varying the values of k_2^0 and k_3 leads to changes in the $Y_{8,\text{max}}$ value.

The set of equations was integrated by the fourth-order Runge–Kutta method with the initial conditions

$Y_i = 0$ and $Y_1 = 1$. The calculations were carried out for $\phi = 0.10\text{--}0.14$, $T_0 = 400\text{--}598$ K, and $P_0 = 0.4\text{--}20.0$ Torr.

It is seen from Figs. 2–5 that the calculated dependences of the parameter $Y_{8,\max}$, which characterizes the maximal concentration of aerosol, on P_0 and T_0 qualitatively agree with the experiment. Analogously to the experiment, the calculation shows that the inhibitor additives that increase P_1 and decrease the rate of flame propagation [24] also increase the initial pressure of aerosol formation and narrow the region of chain–thermal explosion. The calculation describes the nature of the dependence of the relative self-heating value on P_0 . This means that, in the heterophaseous branched chain process, the conditions for the transition of isothermal ignition to the chain–thermal process in self-ignition and the transition from heterogeneous to three-dimensional phase formation are practically equivalent.

Thus, in this work, using DCS oxidation as a sample reaction, we determined the specific features of transition of RCP from the regime of film formation to the regime of aerosol formation and kinetic factors responsible for these specific features.

ACKNOWLEDGMENTS

This work was supported by the Russian Foundation for Basic Research (grant nos. 00-03-3279 and 02-03-32993).

REFERENCES

- Gusev, A.I., *Usp. Fiz. Nauk*, 1998, vol. 163, no. 1, p. 55.
- Brus, E., *J. Chem. Phys.*, 1984, vol. 80, p. 4403.
- Henqlein, A., *Chem. Rev.*, 1989, vol. 89, p. 1861.
- Amelin, A.A., *Teoreticheskie osnovy obrazovaniya tumana iz peresyshchennogo para* (Theoretical Foundation of Fog Formation from Oversaturated Vapor), Moscow: Nauka, 1966.
- Andrievskii, R.A., *Usp. Khim.*, 1994, vol. 63, no. 5, p. 431.
- Khairutdinov, R.F., *Usp. Khim.*, 1998, vol. 67, no. 2, p. 125.
- Azatyany, V.V., Vasil'eva, L.L., Nenasheva, L.A., *et al.*, *Kinet. Katal.*, 1987, vol. 28, no. 5, p. 1068.
- Azatyany, V.V., Lukashov, A.S., Nagornyi, S.S., *et al.*, *Kinet. Katal.*, 1993, vol. 34, no. 3, p. 404.
- Aivazyany, R.G., Azatyany, V.V., and Satunkina, L.F., *Kinet. Katal.*, 1996, vol. 37, no. 2, p. 497.
- Maklakov, S.V., Aivazyany, R.G., Azatyany, V.V., *et al.*, *Mendeleev Commun.*, 1995, no. 1, p. 135.
- Rubtsov, N.M., Tsvetkov, G.I., Azatyany, V.V., and Chernysh, V.I., *Kinet. Katal.*, 2001, vol. 42, no. 2, p. 249.
- Azatyany, V.V., *Kinet. Katal.*, 1977, vol. 18, no. 2, p. 282.
- Azatyany, V.V., *Kinet. Katal.*, 1999, vol. 40, no. 6, p. 818.
- Ryzhkov, O.T., Azatyany, V.V., Rubtsov, N.M., and Temchin, S.M., *Kinet. Katal.*, 1995, vol. 36, no. 1, p. 99.
- Zel'dovich, Ya.B., *Acta Physicochim. URSS*, 1943, vol. 18, p. 11.
- Volmer, M., *Kinetik der Phasenbildung*, Dresden: Steinkopff, 1939.
- Frenkel, J., *Kinetic Theory of Liquids*, New York: Oxford Univ. Press, 1946.
- Matusevich, L.R., *Kristallizatsiya iz rastvorov v khimicheskoi promyshlennosti* (Crystallization from Solutions in Chemical Industry), Moscow: Khimiya, 1968.
- Mikheev, V.V., Laulainen, N.S., Barlow, S.E., *et al.*, *J. Chem. Phys.*, 2000, vol. 113, no. 9, p. 3704.
- Petrov, Yu.I., *Klastery i malye chastitsy* (Clusters and Small Clusters), Moscow: Nauka, 1986, p. 118.
- Shelud'ko, A., Toshev, B.V., and Bojajiev, D.T., *J. Chem. Phys.*, 1957, vol. 26, no. 1, p. 231.
- Wurlitzer, S., Steffen, P., and Fisher, Th.M., *J. Chem. Phys.*, 2000, vol. 112, no. 13, p. 5915.
- Semenov, N.N., *O nekotorykh problemakh khimicheskoi kinetiki i reaktsionnoi sposobnosti* (On Some Problems of Chemical Kinetics and Reactivity), Moscow: Akad. Nauk SSSR, 1958.
- Karpov, V.P., Rubtsov, N.M., Ryzhkov, O.T., *et al.*, *Khim. Fiz.*, 1998, vol. 17, no. 4, p. 73.
- Frank-Kamenetskii, D.A., *Diffuziya i teploperedacha v khimicheskoi kinetike* (Diffusion and Heat Transfer in Chemical Kinetics), Moscow: Nauka, 1967.
- Karpov, V.P., Rubtsov, N.M., Tsvetkov, G.I., and Chernysh, V.I., *Khim. Fiz.*, 2000, vol. 19, no. 8, p. 74.
- Tablitsy fizicheskikh velichin* (Tables of Physical Quantities), Kikoin, I.K., Ed., Moscow: Atomizdat, 1976.
- Azatyany, V.V., Rubtsov, N.M., Ryzhkov, O.T., and Temchin, S.M., *Kinet. Katal.*, 1996, vol. 37, no. 6, p. 805.
- Repinskii, S.M., *Vvedenie v khimicheskuyu fiziku po-verkhnosti tverdykh tel* (Introduction to Chemical Physics of Solid Surfaces), Novosibirsk: Nauka, 1993.